Pergamon

Int. J. Solids Structures Vol. 35, No. 19, pp. 2475–2486, 1998
© 1998 Elsevier Science Ltd
All rights reserved. Printed in Great Britain
0020–7683/98 $19.00 + .00

PII: S0020–7683(97)00145–5

VOID-NUCLEATION VS VOID-GROWTH CONTROLLED PLASTIC FLOW LOCALIZATION IN MATERIALS WITH NONUNIFORM PARTICLE DISTRIBUTIONS

Y. HUANG and A. CHANDRA
Department of Mechanical Engineering—Engineering Mechanics,
Michigan Technological University, Houghton, MI 49931, U.S.A.
E-mail: yyhuang@mtu.edu

and

N. Y. LI
Engineering Design Center, Alcoa Technical Center, Alcoa Center, PA 15069, U.S.A.

(*Received* 19 *May* 1997)

Abstract—Plastic flow localization may occur after significant void growth or immediately after void nucleation. In the present work, a model is developed to investigate the role of nonuniform particle distributions (e.g. random distribution, clusters) in plastic flow localization. A parameter is developed to quantitatively determine whether localization is predominantly controlled by void-nucleation or by void-growth. It is established that, for large clusters of particles, localization is more likely to be initiated by void nucleation, while it is dominated by void growth for small clusters. Both critical strain and stress void-nucleation criteria are investigated. It is observed that void-nucleation governed by the critical stress criterion initiates plastic flow localization at a much lower strain level than that governed by the critical strain criterion. © 1998 Elsevier Science Ltd. All rights reserved.

1. INTRODUCTION

The ductile failure mechanism in most structural metals is the nucleation, growth, and coalescence of microvoids that result from debonding or cracking of second-phase particles. A nonuniform distribution of particles may accelerate this failure process by plastic flow localization in the form of a separation or shear band at a much earlier time or much smaller load, as compared with a uniform particle distribution. Once plastic flow localization occurs, the material inside the band deforms significantly faster than that outside such that further deformation is mainly limited to the band until overall ductility is terminated.

Needleman and Rice (1978) developed the localization criterion for a voided, dilating material within the general framework of plastic flow localization (Rice, 1976). Yamamoto (1978) and Saje *et al.* (1982) investigated an idealized nonuniform void distribution (an infinite planar band with an excess of uniformly distributed voids sandwiched by two uniform blocks of materials). It is observed that the overall ductility is very sensitive to the excess of voids in the band; a 5% excess of void volume fraction in the band results in a factor-of-two reduction of ductility below that for the material with uniform void distribution. However, Boucier *et al.* (1986) and Spitzig *et al.* (1988) observed in their iron compact experiments that the local porosity at clusters of voids is 4–7 times the average porosity, while the measured ductility could only be reproduced by taking the initial porosity in Yamamoto's (1978) and Saje *et al.*'s (1982) infinite band solution to be 1.5–2 times the average porosity. Motivated by this inconsistency, Ohno and Hutchinson (1984) studied a somewhat more realistic nonuniform void distribution, a circular disk-shaped cluster of voids, and established that a small cluster of voids can be severely deleterious at high stress triaxiality. However, at relatively low stress triaxiality such as uniaxial tension, a large cluster of voids [e.g. Yamamoto's (1978) and Saje *et al.*'s (1982) infinite band] gives

significantly loss in ductility as compared to a small cluster. Becker (1987) further carried out a finite element analysis of nonuniform void distribution in accord with patterns measured in a powered-iron compact. He verified that plastic flow localization occurs at a much lower strain in the material with nonuniform void distribution. Similarly, Magnusen *et al.* (1988, 1990) made similar observations from their perforated strip experiments.

For general nonuniform defect distributions, Huang and Hutchinson (1989) showed that *the nonlinear shear localization process is largely controlled by a most critical cluster of defects*. Defects outside this critical cluster has little or no contributions to plastic shear localization, i.e. the difference between plastic shear localization strain for this critical cluster of defects and that accounting for all defects in the nonuniform defect distribution is rather small. A simple scheme to identify this critical cluster and to estimate the plastic shear localization strain was established. Huang (1993) investigated the general plastic flow localization in nonuniform particle distribution under triaxial stress states. For over 250 randomly generated particles distributions, it was verified that the above conclusion on the *most critical cluster of defects* still holds. Accordingly, the issues in nonuniform particle distributions become (1) the identification of the most critical cluster, and (2) the estimation of the corresponding plastic flow localization strain. The first issue is addressed in Huang (1993), while the present paper focuses on the second one.

For a nonuniform particle distribution, plastic flow localization may happen after voids grow significantly and start to coalesce. It can also occur immediately after voids are nucleated, i.e. triggered by void-nucleation. These two circumstances are called void-growth controlled localization and void-nucleation controlled localization, respectively.

2. GENERAL DESCRIPTION OF THE MODEL

Figure 1 shows an example of a nonuniform particle distribution. The second phase particles are uniformly distributed outside the band, as characterized by a constant particle volume fraction f_0. Inside the band there is a circular, disk-shaped cluster of particles, representing a region of nonuniformity in an otherwise uniform material. This band is a potential band for plastic flow localization. Its initial thickness, λ, which enters the analysis as a scale length, is typically on the order of particle spacing.

The nonuniform particle distribution in the band is represented by the following nonuniform particle volume fraction f_p:

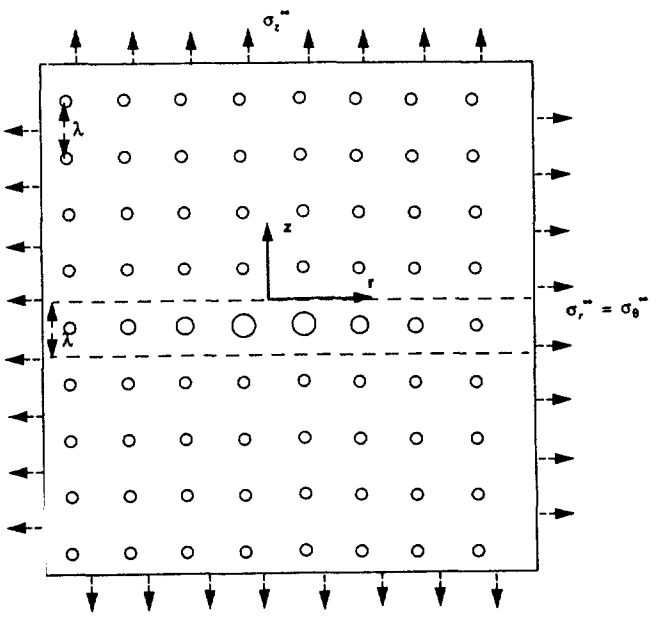

Fig. 1. Conventions.

$$f_p = f_0 + \Delta \exp\left[-\frac{1}{2}\left(\frac{r}{s\lambda}\right)^2\right], \tag{1}$$

where r is the radius to the center of the cluster (Fig. 1), λ is the initial band thickness, $s\lambda$ represents the radius of the cluster, f_0 is the constant particle volume fraction far away from the cluster (also outside the band), and Δ is the maximum excess in particle volume fraction at the center of the cluster over the average particle volume fraction f_0. The limit of $\Delta = 0$ corresponds to an everywhere uniform particle distribution, while the limit of $s = \infty$ represents Yamamoto's (1978) and Saje *et al.*'s (1982) infinite band with uniform excess of defects in the band. This representation of nonuniform particle distribution is similar to Ohno and Hutchinson's (1984) for a cluster of voids.

The material has an elastic-power law stress–strain relation under uniaxial tension,

$$\bar{\sigma} = E\bar{\varepsilon} \quad \text{if} \quad \bar{\varepsilon} \leqslant \sigma_Y/E,$$
$$\bar{\sigma} = \sigma_Y(E\bar{\varepsilon}/\sigma_Y)^N \quad \text{if} \quad \bar{\varepsilon} > \sigma_Y/E, \tag{2}$$

where $\bar{\sigma}$ is the true stress, $\bar{\varepsilon}$ is the logarithmic strain, E is the Young's modulus, σ_Y is the yield stress, and N is the plastic hardening exponent ($0 < N < 1$). The material is subjected to remote axisymmetric tension, $\sigma_r^\infty = \sigma_\theta^\infty = \rho\sigma_z^\infty$, where r and θ are radial and circumferential directions within the band, and the axial direction, z, is normal to the band plane, ρ is the stress triaxiality ratio. The limits of $\rho = 0$ and 1 correspond to remote uniaxial tension and hydrostatic tension, respectively. The orientation of plastic flow localization band may be inclined to z-axis at low stress triaxialities such as uniaxial tension, $\rho = 0$ (Rice, 1976; Yamamoto, 1978; Saje *et al.*, 1982). However, at somewhat higher stress triaxialities, it is anticipated that localization bands are perpendicular to the axis of principal strain. For simplicity, the localization band is assumed to be normal to z axis in the present study.

The remote strains are denoted by ε_r^∞, $\varepsilon_\theta^\infty = \varepsilon_r^\infty$, and ε_z^∞. As the remote loading increases, deformations inside and outside the band are uniform until void nucleation first occurs somewhere in the band due to excess of particles in the band. Once a void is nucleated from a particle in the band, the load carried by the particle is shed to the matrix and nearby particles, which causes further void nucleation from neighboring particles. The continuous void nucleation and growth trigger material softening (Needleman, 1987; Hutchinson and Tvergaard, 1989; Fleck *et al.*, 1989) such that strains inside the band increase much more rapidly than those outside. As pointed out by Needleman and Rice (1978), there exists a critical remote axial strain, at which additional straining in the band can occur without further increase in remote strains. This critical remote axial strain is the plastic flow localization strain and represents the limit of material ductility.

Gurson (1975, 1977) developed the dilatational plasticity, in which voids are "smeared" out and are represented by a continuum variable (local) void volume fraction, f. Nonuniformly distributed voids are, therefore, characterized by a nonuniform void volume fraction. A summary of Gurson model to account for void nucleation is given in the next section.

3. GURSON MODEL

Based on a unit cell analysis, Gurson (1975) derived the dilatational plasticity incorporating void nucleation as well as void growth. The rate of change of the void volume fraction, $\dot{f}$, is composed of contributions from nucleation of new voids, $\dot{f}_n$, and from growth of nucleated voids, $\dot{f}_g$,

$$\dot{f} = \dot{f}_n + \dot{f}_g, \tag{3}$$

where the growth part $\dot{f}_g$ is related to the overall plastic strain-rate $\dot{\varepsilon}_{ij}^p$ by

$$\dot{f}_g = (1-f)\dot{\varepsilon}^p_{kk}, \tag{4}$$

and the nucleation part can be represented by

$$\dot{f}_n = A\dot{\bar{\sigma}} + B\dot{\sigma}_m, \tag{5}$$

where $\bar{\sigma}$ is the flow stress of the matrix material and $\sigma_m = \sigma_{kk}/3$ is the mean stress. The coefficient A characterizes the dependence of void nucleation on plastic deformation, while the coefficient B represents the dependence on the mean stress.

There are two types of criteria for void nucleation [see the review article by Goods and Brown (1979)]. Gurland (1972) suggested that the nucleation of voids is correlated exclusively in terms of the equivalent plastic strain. This can be incorporated in eqn (5) with a vanishing coefficient B, since the equivalent plastic strain is directly related to the matrix flow stress $\bar{\sigma}$ via eqn (1). On the other hand, Argon *et al.* (1975) and Argon and Im (1975) established that void nucleation depends only on the maximum stress transmitted across the particle/matrix interface. This can also be incorporated in Gurson model with coefficients $B = A$, because $\bar{\sigma} + \sigma_m$ is an approximation to this maximum stress (Argon *et al.*, 1975).

On the basis of Gurland's (1972) data on spheroidized carbides in steel, Gurson (1975) found that the coefficient A in eqn (5) is proportional to the volume fraction of unbroken carbide particles. Since void nucleation results from broken particles, the volume fraction of broken particles can be simply estimated by the void volume fraction due to void nucleation, i.e. $\int_0^t \dot{f}_n \, dt$, where the lower and upper limits of integration correspond to the initial, undeformed and the current, deformed states, respectively. The local volume fraction of unbroken particles is $f_p - \int_0^t \dot{f}_n \, dt$, where f_p is the particle volume fraction. Accordingly, the coefficient A is given by

$$A = \psi \left(f_p - \int_0^t \dot{f}_n \, dt \right) \Big/ h \quad \text{if} \quad \int_0^t \dot{f}_n \, dt < f_p, \tag{6}$$

where h is the equivalent plastic hardening modulus of the matrix material,

$$\frac{1}{h} = \frac{d\bar{\varepsilon}^p}{d\bar{\sigma}} = \frac{1}{E}\left[\frac{1}{N} \left(\frac{\bar{\sigma}}{\sigma_Y} \right)^{(1-N)/N} - 1 \right] \quad \text{if} \quad \bar{\sigma} \geqslant \sigma_Y, \tag{7}$$

and the nondimensional coefficient ψ in eqn (6) scales the void nucleation rate. The parameter ψ can be determined from a uniaxial tension experiment since ψf_p is the initial slope in the plot of void volume fraction f vs the axial strain ε. Such experimental curves of f vs ε can be obtained in the literature [e.g. Argon and Im (1975); Argon *et al.* (1975); Fisher and Gurland (1981a, b); Le Roy *et al.* (1981); Brownrigg *et al.* (1983); Boucier *et al.* (1986); Spitzig *et al.* (1988); Walsh *et al.* (1989)]. Typical values of ψ estimated from Walsh *et al.*'s (1989) experiments are on the order of 1. The coefficient A reaches zero once all particles have nucleated voids, and contribution to the rate of change of void volume fraction from void nucleation vanishes thereafter.

In terms of the current effective flow stress $\bar{\sigma}$ in the matrix, Gurson (1975) derived the following yield condition for a voided material based on a unit cell analysis

$$\Phi(\sigma_e, \sigma_{kk}) = \left(\frac{\sigma_e}{\bar{\sigma}} \right)^2 + 2fq_1 \cosh\left(\frac{\sigma_{kk}}{2\bar{\sigma}} \right) - (1 + q_1^2 f^2) = 0, \tag{8}$$

where $\sigma_e = (3\sigma'_{ij}\sigma'_{ij}/2)^{1/2}$ is the effective stress and σ'_{ij} is the stress deviator, $q_1 = 3/2$ following Tvergaard's (1981, 1982) recommendation. This factor of 3/2 is identical to Huang's (1991) modification of Rice and Tracey's (1969) void dilatation rate.

The evolution of the matrix flow stress $\bar{\sigma}$ is determined by equating the overall plastic work rate to the matrix plastic work rate per unit volume,

$$\dot{\bar{\sigma}} = \frac{h}{(1-f)\bar{\sigma}} \sigma_{ij} \dot{\varepsilon}^{\mathrm{p}}_{ij}, \tag{9}$$

where the plastic strain-rates under continued plastic loading are obtained from the normality of inelastic flow to the yield surface,

$$\dot{\varepsilon}^{\mathrm{p}}_{ij} = \Lambda \frac{\partial \Phi}{\partial \sigma_{ij}} \frac{\partial \Phi}{\partial \sigma_{kl}} \dot{\sigma}_{kl}, \tag{10}$$

where $\dot{\sigma}_{kl}$ is the spin-invariant Jaumann stress-rate, the amplitude Λ is determined by the yield surface consistency condition and depends on the effective stress σ_{e}, hydrostatic stress σ_{kk}, flow stress $\bar{\sigma}$, void volume fraction f. In conjunction with the elastic strain-rate

$$\dot{\varepsilon}^{\mathrm{e}}_{ij} = \frac{1+\nu}{E} \dot{\sigma}_{ij} - \frac{\nu}{E} \dot{\sigma}_{kk} \delta_{ij} \tag{11}$$

(ν is Poisson's ratio), the constitutive equation can be inverted to give

$$\dot{\sigma}_{ij} = L_{ijkl} \dot{\varepsilon}_{kl}, \tag{12}$$

where

$$L_{ijkl} = G(\delta_{ik}\delta_{jl} + \delta_{il}\delta_{jk}) + \left(K - \frac{2}{3}G\right)\delta_{ij}\delta_{kl} - \frac{1}{H}\left(G\frac{\sigma'_{ij}}{\sigma} + K\alpha\delta_{ij}\right)\left(G\frac{\sigma'_{kl}}{\bar{\sigma}} + K\gamma\delta_{kl}\right), \tag{13}$$

with $G = E/(2+2\nu)$ and $K = E/(3-6\nu)$ being elastic shear and bulk moduli, δ_{ij} being the Kroneker δ, and

$$\alpha = \frac{3f}{4}\sinh\left(\frac{\sigma_{kk}}{2\bar{\sigma}}\right), \quad \beta = \frac{3}{2}\cos h\left(\frac{\sigma_{kk}}{2\bar{\sigma}}\right) - \frac{9f}{4}, \quad \gamma = \alpha + \frac{B}{3}\bar{\sigma}\beta,$$

$$H = \frac{h}{9(1-f)}\left[\left(\frac{\sigma_{\mathrm{e}}}{\bar{\sigma}}\right)^2 + \alpha\frac{\sigma_{kk}}{\bar{\sigma}}\right]\left[\left(\frac{\sigma_{\mathrm{e}}}{\bar{\sigma}}\right)^2 + \alpha\frac{\sigma_{kk}}{\bar{\sigma}} - A\bar{\sigma}\beta\right] - \frac{1-f}{3}\bar{\sigma}\alpha\beta + \frac{G}{3}\left(\frac{\sigma_{\mathrm{e}}}{\bar{\sigma}}\right)^2 + K\alpha\gamma. \tag{14}$$

It is observed that the incremental moduli do not have symmetry, $L_{ijkl} \neq L_{klij}$, unless the coefficient B is zero, corresponding to the critical strain void-nucleation criterion.

4. PLASTIC FLOW LOCALIZATION

The Gurson model (1975), incorporating both void nucleation and void growth as summarized in the previous section, is used to characterize materials inside as well as outside the band. This is not inappropriate because the Gurson model was derived from the analysis of a unit cell that contains a single void, which is consistent with the identification of initial thickness of the band as the average particle spacing in the present study. This is similar to Ohno and Hutchinson's (1984) analysis for nonuniform void distributions.

It is useful to cast the rate equations in terms of the updated nominal stress-rate $\dot{n}_{ij}$, which is related to the Jaumann rate $\dot{\sigma}_{ij}$ by

$$\dot{n}_{ij} = \dot{\sigma}_{ij} - \sigma_{ik}\Omega_{kj} - \dot{\varepsilon}_{ik}\sigma_{kj} + \dot{\varepsilon}_{kk}\sigma_{ij}, \tag{15}$$

where the spin tensor Ω_{ij} and strain-rate $\dot{\varepsilon}_{ij}$ are related to displacement-rate $\dot{u}_i$ by

$$\Omega_{ij} = (\dot{u}_{i,j} - \dot{u}_{j,i})/2, \quad \dot{\varepsilon}_{ij} = (\dot{u}_{i,j} + \dot{u}_{j,i})/2. \tag{16}$$

The incremental equilibrium equation is

$$\dot{n}_{ij,i} = 0. \tag{17}$$

The deformation inside and outside the band is analyzed separately, and coupled together through the continuity conditions at the band boundary. Follow Ohno and Hutchinson (1984), Huang and Hutchinson (1989), and Huang (1993), two approximations are made to simplify the analysis without altering the characteristic nature of the problem. First, stresses and strains in the band are averaged along the band thickness direction, and are therefore independent of the axial coordinate z. The out-of-plane shear stress, σ_{zr} and $\sigma_{z\theta}$, and shear strains, ε_{zr} and $\varepsilon_{z\theta}$, vanish due to anti-symmetry. The normal stress-rate $\dot{n}^{b}_{zz}$ in the band is the only non-zero traction-rate at the interface between materials inside and outside the band, and it is related to non-zero strain-rates $\dot{\varepsilon}^{b}_{rr}$, $\dot{\varepsilon}^{b}_{\theta\theta}$, and $\dot{\varepsilon}^{b}_{zz}$ in the band by eqn (15) at each instant in the deformation history, i.e.

$$\dot{n}^{b}_{zz} = (L^{b}_{zzrr} + \sigma^{b}_{zz})\dot{\varepsilon}^{b}_{rr} + (L^{b}_{zz\theta\theta} + \sigma^{b}_{zz})\dot{\varepsilon}^{b}_{\theta\theta} + L^{b}_{zzzz}\dot{\varepsilon}^{b}_{zz}. \tag{18}$$

The first approximation is justified as long as the thickness of the band λ is small compared to the in-plane dimension of the particle cluster, i.e. $s \gg 1$.

The deformation outside the band is analyzed separately. At each instant in the deformation history, the material outside the band is subjected to remote nominal axial and radial stress-rates, $\dot{n}^{\infty}_{zz}$ and $\dot{n}^{\infty}_{rr}$, and the normal stress-rate $\dot{n}^{b}_{zz}$ at the band boundary, where the remote nominal stress-rates are prescribed with a fixed stress triaxiality ratio, $\rho = \dot{\sigma}^{\infty}_{rr}/\dot{\sigma}^{\infty}_{zz}$. The displacement-rate outside the band can be decomposed into that associated with uniform stress-rates $(\dot{n}^{\infty}_{rr}, \dot{n}^{\infty}_{zz})$ and that corresponding to a half-space subjected to a distributed normal traction-rate, $\dot{n}^{b}_{zz} - \dot{n}^{\infty}_{zz}$, on the boundary of the half-space. Follow Ohno and Hutchinson (1984), the second assumption is made that the spatial variations of incremental moduli outside the band are neglected and the increment moduli are approximated by corresponding moduli associated with the remote field, i.e. L^{∞}_{ijkl}. This assumption is not unreasonable because particles are uniformly distributed outside the band such that the spatial variations of incremental moduli are mainly limited to regions close to the cluster of particles in the band. It results in overly stiff material near the cluster where the higher stress levels would induce relatively lower incremental moduli. However, based on their agreement with Abeyaratne and Triantafyllidis' (1981) study on plastic flow localization, Ohno and Hutchinson (1984) pointed out that this type of approximation may not be too significant. Therefore, the relation between nominal stress-rates and strain-rates, eqn (15), becomes

$$\begin{bmatrix} \dot{n}_{rr} \\ \dot{n}_{\theta\theta} \\ \dot{n}_{zz} \end{bmatrix} = \begin{bmatrix} L^{\infty}_{1111} & L^{\infty}_{1122} + \sigma^{\infty}_{rr} & L^{\infty}_{1133} + \sigma^{\infty}_{rr} \\ L^{\infty}_{1122} + \sigma^{\infty}_{rr} & L^{\infty}_{1111} & L^{\infty}_{1133} + \sigma^{\infty}_{rr} \\ L^{\infty}_{3311} + \sigma^{\infty}_{zz} & L^{\infty}_{3311} + \sigma^{\infty}_{zz} & L^{\infty}_{3333} \end{bmatrix} \begin{bmatrix} \dot{\varepsilon}_{rr} \\ \dot{\varepsilon}_{\theta\theta} \\ \dot{\varepsilon}_{zz} \end{bmatrix} \tag{19}$$

for materials outside the band, where

$$L^{\infty}_{1111} = L^{\infty}_{rrrr} = L^{\infty}_{\theta\theta\theta\theta}, \quad L^{\infty}_{1122} = L^{\infty}_{rr\theta\theta} = L^{\infty}_{\theta\theta rr},$$
$$L^{\infty}_{1133} = L^{\infty}_{rrzz}, \quad L^{\infty}_{3311} = L^{\infty}_{zzrr}, \quad \text{and} \quad L^{\infty}_{3333} = L^{\infty}_{zzzz}.$$

From eqn (19), the uniform remote strain-rates are given by

$$\begin{bmatrix} \dot{\varepsilon}_{rr}^{\infty} = \dot{\varepsilon}_{\theta\theta}^{\infty} \\ \dot{\varepsilon}_{zz}^{\infty} \end{bmatrix} = \begin{bmatrix} L_{1111}^{\infty} + L_{1122}^{\infty} + \sigma_{rr}^{\infty} & L_{1133}^{\infty} + \sigma_{rr}^{\infty} \\ 2(L_{3311}^{\infty} + \sigma_{zz}^{\infty}) & L_{3333}^{\infty} \end{bmatrix}^{-1} \begin{bmatrix} \dot{n}_{rr}^{\infty} \\ \dot{n}_{zz}^{\infty} \end{bmatrix}. \tag{20}$$

It is observed that eqn (19) is similar to stress–strain relation for an elastic, transversely isotropic solid. Along the lines indicated by Elliott (1948, 1949), Huang (1990) found the analogue of Boussinesq solution (a normal unit force on the boundary of a half-space) for a material with a constitutive relation given by eqn (19). The Green's function, $K_i(x, y, z)$ for the displacement-rates is obtained for a unit normal force at the origin. Accordingly, for uniform remote stress-rates $(\dot{n}_{rr}^{\infty}, \dot{n}_{zz}^{\infty})$ and $\dot{n}_{zz}^{b}$ on the band boundary, the displacement-rates outside the band can be expressed in terms of Green's functions as

$$\begin{bmatrix} \dot{u}_x(x, y, z) \\ \dot{u}_y(x, y, z) \\ \dot{u}_z(x, y, z) \end{bmatrix} = \begin{bmatrix} \dot{\varepsilon}_{rr}^{\infty} x \\ \dot{\varepsilon}_{rr}^{\infty} y \\ \dot{\varepsilon}_{zz}^{\infty} z \end{bmatrix} + \int \begin{bmatrix} [\dot{n}_{zz}^{b}(\xi, \eta) - \dot{n}_{zz}^{\infty}] K_x(x-\xi, y-\eta, z) \\ [\dot{n}_{zz}^{b}(\xi, \eta) - \dot{n}_{zz}^{\infty}] K_y(x-\xi, y-\eta, z) \\ [\dot{n}_{zz}^{b}(\xi, \eta) - \dot{n}_{zz}^{\infty}] K_z(x-\xi, y-\eta, z) \end{bmatrix} \mathrm{d}\xi \, \mathrm{d}\eta, \tag{21}$$

where the integration is over the entire band boundary.

The analyses for material inside and outside the band are coupled together through continuity of displacement-rates at the band boundary. This can be written as

$$\dot{u}_r^{b} = \dot{\varepsilon}_{rr}^{\infty} r + \int [\dot{n}_{zz}^{b}(\xi, \eta) - \dot{n}_{zz}^{\infty}][K_x(x-\xi, y-\eta, 0)\cos\theta + K_y(x-\xi, y-\eta, 0)\sin\theta] \, \mathrm{d}\xi \, \mathrm{d}\eta, \tag{22}$$

and

$$\dot{\varepsilon}_{zz}^{b}(r)\lambda \exp[\varepsilon_{zz}^{b}(r)] = \dot{\varepsilon}_{zz}^{\infty}\lambda \exp(\varepsilon_{zz}^{\infty}) + 2\int [\dot{n}_{zz}^{b}(\xi, \eta) - \dot{n}_{zz}^{\infty}][K_z(x-\xi, y-\eta, 0) \, \mathrm{d}\xi \, \mathrm{d}\eta. \tag{23}$$

Equation (23) states that the rate of thickness increase at any point in the band over the corresponding rate at infinity must equal the additional separation-rate of the face of the half-space. Using the relation between strain-rates and displacement-rates in eqn (16), one finds the strain-rates $\dot{\varepsilon}_{rr}^{b}$ and $\dot{\varepsilon}_{\theta\theta}^{b}$ in the band in terms of $\dot{n}_{zz}^{b} - \dot{n}_{zz}^{\infty}$, while the other non-zero strain-rate $\dot{\varepsilon}_{zz}^{b}$ in the band is given in terms of $\dot{n}_{zz}^{b} - \dot{n}_{zz}^{\infty}$ in eqn (23). The substitution of strain-rates into eqn (18) yields the following integral equation for the normal stress-rate $\dot{n}_{zz}^{b}$,

$$\begin{aligned} &[1 - \alpha(L_{zzrr}^{b} + \sigma_{zz}^{b})][\dot{n}_{zz}^{b}(r) - \dot{n}_{zz}^{\infty}] + \alpha_1 (L_{zzrr}^{b} - L_{zz\theta\theta}^{b}) r^{-2} \int_0^r \zeta [\dot{n}_{zz}^{b}(\xi) - \dot{n}_{zz}^{\infty}] \, \mathrm{d}\zeta \\ &\quad - 2\alpha_3 L_{zzzz}^{b} \lambda^{-1} \exp(-\varepsilon_{zz}^{b}) \int_0^{\infty} [\dot{n}_{zz}^{b}(\zeta) - \dot{n}_{zz}^{\infty}] F(\zeta/r) \, \mathrm{d}\zeta \\ &\quad = [L_{zzrr}^{b} + L_{zz\theta\theta}^{b} - 2L_{3311}^{\infty} + 2(\sigma_{zz}^{b} - \sigma_{zz}^{\infty})]\dot{\varepsilon}_{rr}^{\infty} + [\exp(\varepsilon_{zz}^{\infty} - \varepsilon_{zz}^{b}) L_{zzzz}^{b} - L_{3333}^{\infty}]\dot{\varepsilon}_{zz}^{\infty} \end{aligned} \tag{24}$$

where function F and parameters α_1 and α_3 are given in the Appendix. At each instant in the loading history, eqn (24) is solved numerically, and stresses, strains, void volume fraction, and incremental moduli are then updated.

Plastic flow localization occurs when eqn (24) starts to have a non-trivial solution for vanishing remote strain-rates (Rice, 1976; Needleman and Rice, 1978; Ohno and Hutchinson, 1984). At this moment, additional straining in the band can occur without further increase in the remote strain. This corresponding remote axial strain is the plastic flow localization strain, ε_L.

5. RESULTS AND DISCUSSION

The present study focuses on two key variables, the plastic flow localization strain, ε_L, and the contribution to void volume fraction from void nucleation at plastic flow localization, as defined by

$$\chi = \int_0^t \dot{f}_n \, dt/f. \tag{25}$$

If $\chi \ll 1$, the contribution from void nucleation to the void volume fraction is small such that plastic flow localization is void-growth controlled. If $\chi \sim 1$, void nucleation dominates the contribution to the void volume fraction, and localization is triggered by void nucleation.

Results are presented for typical material parameters: plastic hardening exponent $N = 0.1$, the ratio of yield stress to Young's modulus $\sigma_Y/E = 0.0033$, Poisson's ratio $\nu = 0.3$. The particle volume fraction outside the band is taken as 1% ($f_0 = 0.01$), while the coefficient ψ characterizing the void nucleation rate in eqn (6) is $\psi = 3$ estimated from Walsh *et al.*'s (1989) experiments.

The effect of stress triaxiality on plastic flow localization has been thoroughly studied by Ohno and Hutchinson (1984). At high stress triaxiality levels (e.g. $\rho = 0.5$ or 0.65), which are characteristic of situations where plastic flow occurs under highly constrained conditions such as the tip of a plane strain crack, it has been established that a small cluster can be as deleterious as the infinite band results. In the present study, the stress triaxiality ratio is fixed at a relatively low level, $\rho = 0.25$, such that focus is on parameters characterizing the nonuniform particle distributions (e.g. the normalized size s of the particle cluster, the maximum excess Δ in particle volume fraction in the band). It is observed that the stress triaxiality ratio $\rho = 0.25$ is not untypical of values at the necked down section of a rounded tensile bar just prior to localization.

The plastic flow localization strain ε_L is shown versus the maximum excess in particle volume fraction Δ in Fig. 2 for various sizes of particle clusters at $\rho = 0.25$. The critical-strain void nucleation criterion is used [i.e. $B = 0$ in eqn (5)]. For a large cluster ($s = 100$), the localization strain decreases rapidly as Δ increases, in agreement with the infinite band calculation (Yamamoto, 1978; Saje *et al.*, 1982). For a small cluster ($s = 3$), however, the maximum excess in particle volume fraction has little or no effect on localization strain because the localization strain for $s = 3$ is insensitive to Δ. This difference results from the

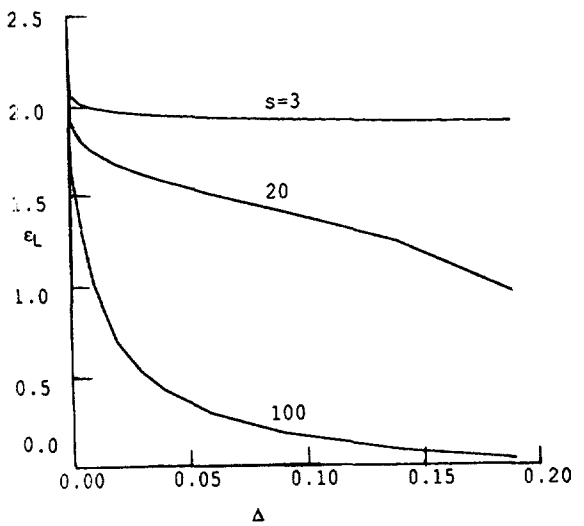

Fig. 2. The plastic flow localization strain, ε_L, vs the maximum excess in particle volume fraction, Δ, for small ($s = 3$), medium ($s = 20$) and large ($s = 100$) clusters of particles at stress triaxiality ratio $\rho = 0.25$.

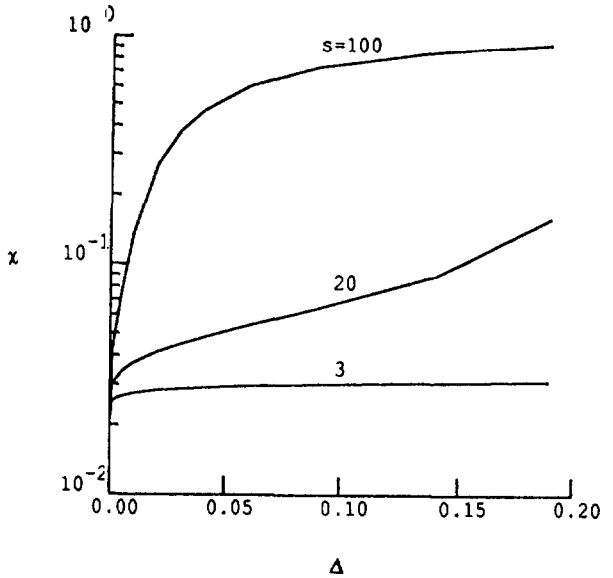

Fig. 3. The contribution to void volume fraction from void nucleation, χ, at the center of the cluster when localization occurs vs the maximum excess in particle volume fraction, Δ, for small ($s = 3$), medium ($s = 20$) and large ($s = 100$) clusters of particles at stress triaxiality ratio $\rho = 0.25$.

role of void nucleation for small and large particle clusters. As shown in Fig. 3, the contribution to the void volume fraction from void nucleation, χ, at the center of the cluster when localization occurs is plotted versus the maximum excess Δ in particle volume fraction. For a small cluster ($s = 3$), χ is only around 2%, corresponding to the void-growth controlled plastic flow localization. For a large cluster ($s = 100$), however, χ rapidly approaches 1 as Δ increases, indicating that the plastic flow localization is triggered by void nucleation.

The plastic flow localization strain ε_L is shown versus the maximum excess in particle volume fraction Δ in Fig. 4 for both critical strain ($B = 0$) and critical stress ($B = A$) void

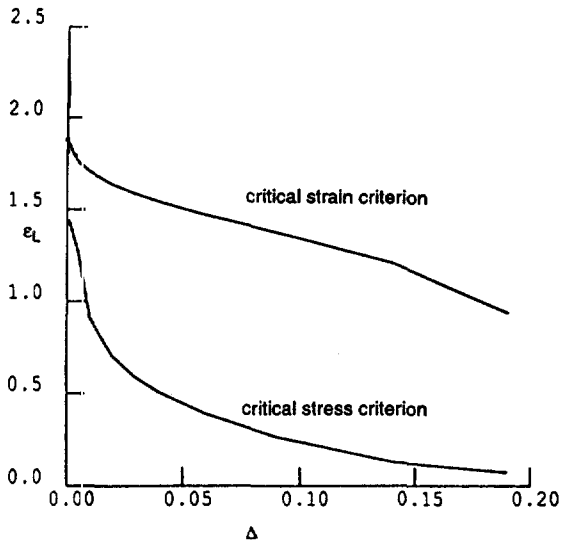

Fig. 4. The plastic flow localization strain, ε_L, vs the maximum excess in particle volume fraction, Δ, for the critical strain and critical stress void nucleation criteria, where normalized cluster size $s = 20$, and stress triaxiality ratio $\rho = 0.25$.

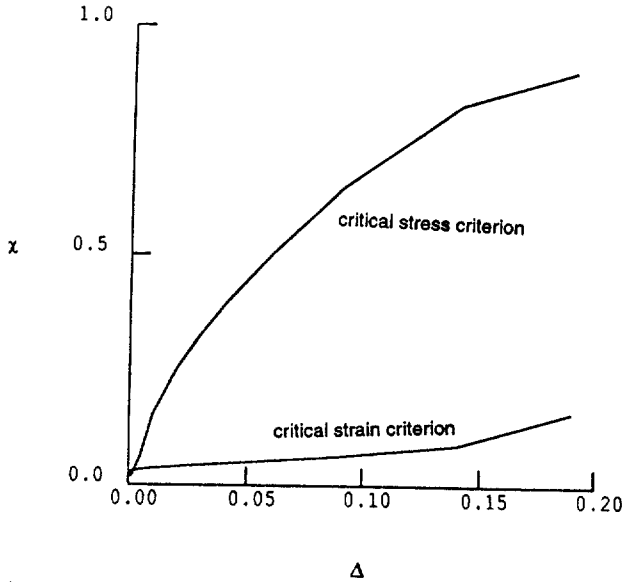

Fig. 5. The contribution to void volume fraction from void nucleation, χ, at the center of the cluster when localization occurs vs the maximum excess in particle volume fraction, Δ, for the critical strain and critical stress void nucleation criteria, where the normalized cluster size $s = 20$, and stress triaxiality ratio $\rho = 0.25$.

nucleation criteria for a medium size particle cluster ($s = 20$) at stress triaxiality ratio $\rho = 0.25$. The plastic flow localization occurs much earlier for the critical stress void nucleation criterion since void nucleation tends to dominate the contribution to void volume fraction. This is clearly observed in Fig. 5 where the contribution to the void volume fraction from void nucleation, χ, at the center of the cluster is plotted versus the maximum excess Δ in particle volume fraction. While χ remains less than 20% for the critical strain void nucleation criterion, it is significantly larger and close to 100% for the critical stress void nucleation criterion, especially for large excess in particle volume fraction.

6. CONCLUDING REMARKS

A model has been developed to investigate the role of random particle distributions and particle clusters in plastic flow localization. The parameter χ in eqn (25) is identified to distinguish void-nucleation and void-growth controlled plastic flow localization. It is established that localization is likely to be triggered by void nucleation for large clusters of particles, and dominated by void growth for small clusters. Void nucleation governed by the critical stress criterion will trigger plastic flow localization at a much lower strain level than that governed by the critical strain criterion. For small particle clusters, localization is insensitive to the maximum excess in local particle volume fraction.

Conclusions based on the model are tempered by the fact that this is an idealized model. The band is assumed to be perpendicular to the direction of maximum principal strain, though the localization band is more likely to be inclined to the axis of principal strain at low stress triaxiality [e.g. Rice (1976); Needleman and Rice (1978); Yamamoto (1978); Saje *et al.* (1982)], as observed in porous media (Needleman and Kushner, 1990), in an aluminum sheet (Becker and Smelser, 1994), and in ductile fracture (Geltmacher *et al.*, 1996). Therefore, the model may overestimate the plastic flow localization strain.

Acknowledgement—YH gratefully acknowledges many helpful discussions with Dr J. W. Hutchinson. The financial support from the National Science Foundation (Grants no. INT-94-23964 and no. CMS-95-22147) and the ALCOA Foundation is acknowledged.

REFERENCES

Abeyaratne, R. and Triantafyllidis, N. (1981) The emergence of shear bands in plane strain. *International Journal of Solids and Structures* **17,** 1113.

Argon, A. S. and Im, J. (1975) Separation of second phase particles in spheroidized 1045 steel, Cu–0.6Pct Cr alloy and maraging steel in plastic straining. *Metallurgical Transactions* **6A,** 839.

Argon, A. S., Im, J. and Safoglu, R. (1975) Cavity formation from inclusions in ductile fracture. *Metallurgical Transactions* **6A,** 825.

Becker, R. (1987) The effect of porosity distribution on ductile failure. *Journal of Mechanics and Physics of Solids* **35,** 577.

Becker, R. and Smelser, R. E. (1994) Simulation of strain localization and fracture between holes in an aluminum sheet. *Journal of Mechanics and Physics of Solids* **42,** 773–790.

Boucier, R. J., Koss, D. A., Smelser, R. E. and Richmond, O. (1986) The influence of porosity on the deformation and fracture of alloys. *Acta Metallica Materiala* **34,** 2443.

Brownrigg, A., Spitzig, W. A., Richmond, O., Teirlinck, D. and Embury, J. D. (1983) The influence of hydrostatic pressure of the flow stress and ductility of a spheroidized 1045 steel. *Acta Metallica* **31,** 1141.

Elliott, H. A. (1948) Three-dimensional stress distributions in hexagonal aeolotropic crystals. *Proceedings of Cambridge Philosophical Society* **44,** 522.

Elliott, H. A. (1949) Axial symmetric stress distributions in aeolotropic hexagonal crystals. The problem of the plane and related problems. *Proceedings of Cambridge Philosophical Society* **45,** 621.

Fisher, J. R. and Gurland, J. (1981a) Void nucleation in spheroidized carbon steels. Part 1: experiments. *Materials Science* **15,** 185.

Fisher, J. R. and Gurland, J. (1981b) Void nucleation in spheroidized carbon steels. Part 1: model. *Materials Science* **15,** 193.

Fleck, N. A., Hutchinson, J. W. and Tvergaard, V. (1989) Softening by void nucleation and growth in tension and shear. *Journal of Mechanics and Physics of Solids* **37,** 515.

Geltmacher, A. B., Koss, D. A., Matic, P. and Stout, M. G. (1996) A modeling study of the effect of stress state on void linking during ductile fracture. *Acta Metallica* **44,** 2201–2210.

Goods, S. H. and Brown, L. M. (1979) The nucleation of cavities by plastic deformation. *Acta Metallica* **27,** 1.

Gurland, J. (1972) Observations on the fracture of cementite particles in a spheroidized 1.05% C steel deformed at room temperature. *Acta Metallica* **20,** 735.

Gurson, A. L. (1975) Plastic flow and fracture behavior of ductile materials incorporating void nucleation, growth and interaction. Ph.D. thesis, Brown University.

Gurson, A. L. (1977) Continuum theory of ductile rupture by void nucleation and growth: part 1—yield criteria and flow rules for porous ductile media. *Journal of Engineering Material Technology* **99,** 2.

Huang, Y. (1990) Cavitation and localization in plastic flow. Ph.D. dissertation, Harvard University, Cambridge, MA.

Huang, Y. (1991) Accurate dilatation rate for spherical voids in triaxial stress fields. *Journal of Applied Mechanics* **58,** 1084.

Huang, Y. (1993) The role of nonuniform particle distribution in plastic flow localization. *Mechanics Material* **16,** 265.

Huang, Y. and Hutchinson, J. W. (1989) A model study of the role of nonuniform defect distribution on plastic shear localization. *Role of Modeling in Materials Design*, ed. J. D. Embury. AIME, p. 129.

Hutchinson, J. W. and Tvergaard, V. (1989) Softening due to void nucleation in metals. In *Fracture Mechanics: Perspectives and Directions*, ASTM STP 1020, eds R. P. Wei and R. P. Gangloff. ASTM, p. 61.

Le Roy, G., Embury, J. D., Edward, G. and Ashby, M. F. (1981) A model of ductile fracture based on the nucleation and growth of voids. *Acta Metallica* **29,** 1509.

Magnusen, P. E., Dubensky, E. M. and Koss, D. A. (1988) The effect of void arrays on void linking during ductile fracture. *Acta Metallica* **36,** 1503.

Magnusen, P. E., Srolovit, D. J. and Koss, D. A. (1990) A simulation of void linking during ductile microvoid fracture. *Acta Metallica* **38,** 1013–1022.

Needleman, A. (1987) A continuum model for void nucleation by inclusion debonding. *Journal of Applied Mechanics* **54,** 525.

Needleman, A. and Kushner, A. S. (1990) An analysis of void distribution effects on plastic flow in porous solids. *European Journal of Mechanics, A/Solids* **19,** 193–206.

Needleman, A. and Rice, J. R. (1978) Limits on ductility set by plastic flow localization. In *Mechanics and Sheet Metal Forming*, eds D. P. Koistinen and N.-M. Wang. Plenum, New York, p. 237.

Ohno, N. and Hutchinson, J. W. (1984) Plastic flow localization due to non-uniform void distribution. *Journal of Mechanics and Physics of Solids* **32,** 63–85.

Rice, J. R. (1976) The localization of plastic deformation. In *Proceedings of the XIVth International Congress of Theoretical and Applied Mechanics*, ed. W. T. Koiter. Delft, North-Holland, Vol. 1, p. 207.

Rice, J. R. and Tracey, D. M. (1969) On the ductile enlargement of voids in triaxial stress fields. *Journal of Mechanics and Physics of Solids* **17,** 201.

Saje, M., Pan, J. and Needleman, A. (1982) Void nucleation effects on shear localization in porous plastic solids. *International Journal of Fracture* **19,** 163.

Spitzig, W. A., Smelser, R. E. and Richmond, O. (1988) The evolution of damage and fracture in iron compacts with various initial porosities. *Acta Metallica Materiala* **36,** 1201.

Tvergaard, V. (1981) Influence of voids on shear band instabilities under plane strain conditions. *International Journal of Fracture* **17,** 389.

Tvergaard, V. (1982) On localization in ductile materials containing spherical voids. *International Journal of Fracture* **18,** 237.

Tvergaard, V. (1990) Material failure by void growth to coalescence. In *Advances in Applied Mechanics*, eds J. W. Hutchinson and V. Tvergaard, Vol. 27, p. 83.

Walsh, J. A., Jata, K. V. and Starke, E. A. (1989) The influence of Mn dispersoid content and stress state on ductile fracture of 2134 type Al-alloys. *Acta Metallica* **37,** 2861–2871.

Yamamoto, H. (1978) Conditions for shear localization in ductile fracture of void containing materials. *International Journal of Fracture* **14**, 347.

APPENDIX

Details of the derivation for eqn (24) can be found in Huang (1990). The function F in eqn (24) is given by

$$F(\zeta) = \zeta\left\{1+\sum_{m=1}^{\infty}\frac{[(2m)!]^2}{2^{4m}(m)!^4}\zeta^{2m}\right\} \quad \text{if} \quad 0 \leqslant \zeta \leqslant 1$$

$$= 1+\sum_{m=1}^{\infty}\frac{[(2m)!]^2}{2^{4m}(m)!^4}\zeta^{-2m} \quad \text{if} \quad \zeta > 1. \tag{A1}$$

Parameters α_1 and α_3 are given by

$$\alpha_1 = \frac{-\mathrm{Im}\left\{\left[(1+k)\left(G-\frac{1}{2}\sigma_{rr}^{\infty}\right)+\frac{1}{2}(1-k)\sigma_{zz}^{\infty}\right]\bar{\mu}^{1/2}\right\}}{\mathrm{Im}\left\{\left[(1+k)\left(G-\frac{1}{2}\sigma_{rr}^{\infty}\right)+\frac{1}{2}(1-k)\sigma_{zz}^{\infty}\right]\bar{\mu}^{1/2}\left(\frac{\bar{k}}{\bar{\mu}}L_{3333}^{\infty}-L_{3311}^{\infty}-\sigma_{zz}^{\infty}\right)\right\}}, \tag{A2}$$

and

$$\alpha_3 = \frac{\left(G-\frac{1}{2}\sigma_{rr}^{\infty}+\frac{1}{2}\sigma_{zz}^{\infty}\right)\mathrm{Im}(k)}{\mathrm{Im}\left\{\left[(1+k)\left(G-\frac{1}{2}\sigma_{rr}^{\infty}\right)+\frac{1}{2}(1-k)\sigma_{zz}^{\infty}\right]\bar{\mu}^{1/2}\left(\frac{\bar{k}}{\bar{\mu}}L_{3333}^{\infty}-L_{3311}^{\infty}-\sigma_{zz}^{\infty}\right)\right\}}, \tag{A3}$$

where G is the elastic shear modulus, Im( ) and $\overline{(\ )}$ stand for the imaginary and conjugate of a complex variable ( ), respectively, k and μ are related by

$$k = \frac{\mu L_{1111}^{\infty}-G-\Delta_1}{L_{1133}^{\infty}+G-\Delta_1} \tag{A4}$$

with $\Delta_1 = (\sigma_{zz}^{\infty}-\sigma_{rr}^{\infty})/2$, and μ and $\bar{\mu}$ are roots of the following quadratic equation

$$a\mu^2+b\mu+c = 0, \tag{A5}$$

where

$$a = L_{1111}^{\infty}(G-\Delta_1),$$

$$b = L_{1133}^{\infty}L_{3311}^{\infty}+L_{1133}^{\infty}(G+\Delta_1)+L_{3311}^{\infty}(G-\Delta_1)-L_{1111}^{\infty}L_{3333}^{\infty},$$

$$c = L_{3333}^{\infty}(G+\Delta_1). \tag{A6}$$